

A functional MRI study of visual oddball: evidence for frontoparietal dysfunction in subjects at risk for alcoholism

Madhavi Rangaswamy,^a Bernice Porjesz,^{a,*} Babak A. Ardekani,^{b,c} Steven J. Choi,^d Jody L. Tanabe,^e Kelvin O. Lim,^f and Henri Begleiter^a

^aDepartment of Psychiatry, SUNY Health Sciences Center at Brooklyn, State University of New York, Brooklyn, NY 11203, USA

^bCenter for Advanced Brain Imaging, Nathan Kline Institute for Psychiatric Research, Orangeburg, NY 10962, USA

^cDepartment of Psychiatry, New York University School of Medicine, New York, NY, USA

^dDepartment of Cardiology, Mount Sinai School of Medicine, New York, NY, USA

^eDepartment of Radiology, University of Colorado Health Sciences Center, Denver, CO, USA

^fDepartment of Psychiatry, University of Minnesota, Minneapolis, MN, USA

Received 5 June 2003; revised 30 July 2003; accepted 5 September 2003

Attending to rare stimuli interspersed among repetitive frequent stimuli produces a positive scalp potential at 300 to 600 ms after the target stimulus onset; this potential is known as the P300 wave. Although there is clear evidence of low visual P300 in subjects at high risk (HR) for developing alcoholism, the functional neuroanatomical correlates have not been studied. Functional and high-resolution anatomical magnetic resonance images were collected during the performance of a visual oddball task, from six control (low risk—LR) subjects with high P300s and eight HR subjects with low P300s. All the HR subjects were offspring of male alcoholics. The data were analyzed using a randomization-based statistical method that accounts for multiple comparisons, requires no assumptions about the noise structure of the data, and does not require spatial or temporal smoothing. Target counts showed that all subjects performed the task comparably. Analysis of the functional magnetic resonance imaging (fMRI) data revealed two areas with significantly lower activation in the HR group when compared to the LR group: the bilateral inferior parietal lobule (BA 40), and the bilateral inferior frontal gyrus (BA 44). Inferior parietal lobule showed significantly lower activation in the HR group in contrast to the LR group, and inferior frontal gyrus was not activated in the HR group but was only activated in the LR group. This finding indicates that a dysfunctional frontoparietal circuit may underlie the low P300 responses seen in HR subjects. This perhaps implies a deficiency in the rehearsal component of the working memory system.

© 2003 Elsevier Inc. All rights reserved.

Keywords: Alcoholism; Frontoparietal dysfunction; P300

Introduction

Neuropsychological deficits in chronic alcoholism have been well documented, especially in spatial working memory, problem solving, and cognitive flexibility (Nixon et al., 1995; Oscar-Berman and Hutner, 1993; Sullivan et al., 1993). Supporting functional evidence indicates that a diminished activation of the frontal cortical system probably underlies attention and visual working memory deficits in chronic alcoholics (Pfefferbaum et al., 2001). In the case of offspring of alcoholics, deficits in visuospatial skills, verbal performance, categorization or organization, attention, and memory indices have been consistently reported (for a review, see Nixon and Tivis, 1997); this detailed review also suggests that these cognitive deficits can predate chronic alcohol use. Existing neuroanatomical studies in offspring of alcoholics, who are at high risk, are few. In a pharmacological challenge study using positron emission tomography (PET), cerebellar function was implicated in the sensitivity to alcohol and benzodiazepines in high-risk subjects (Volkow et al., 1995). Another study, using magnetic resonance imaging, examined cerebral, amygdala, and hippocampal volumes in high-risk adolescent and young adult offspring from multiplex alcoholism families and age-, gender-, and IQ-matched control subjects without a family history for alcoholism or other substance dependence (Hill et al., 2001). The authors found smaller right amygdala volumes in high-risk subjects and this was correlated with the amplitude of the P300 wave.

In cognitive tasks where infrequent target stimuli are embedded in a series of frequent stimuli, target detection elicits large positive component 300 to 600 ms after stimulus onset, called the P300 or P3. The amplitude of this component is highest parietally (Sutton et al., 1965). The P300 is elicited when the subjects attend to and discriminate the stimulus features (Polich and Bondurant, 1997) and is influenced by the probability of the event irrespective of the task relevance (Duncan-Johnson and Donchin, 1977). P300 has been proposed to reflect processes of attentional allocation and the process of context updating in the working memory involved with the match–mismatch of the visual stimulus with the stored

* Corresponding author. Department of Psychiatry, SUNY Health Sciences Center at Brooklyn, State University of New York, Box 1203, 450 Clarkson Avenue, Brooklyn, NY, 11203. Fax: +1-718-270-4081.

E-mail address: bp@ens.hscbklyn.edu (B. Porjesz).

Available online on ScienceDirect (www.sciencedirect.com).

representation (Donchin and Coles, 1988; Polich and Herbst, 2000) and possibly cognitive closure (Verleger, 1988). Some authors have argued that stimulus categorization is more important than stimulus probability for the P300 amplitude (Mecklinger and Ullsperger, 1993; Nasman and Rosenfeld, 1990). The amplitude of the P300 is believed to reflect probability and evaluation of the stimulus and the latency reflects the mental processing speed (Polich and Herbst, 2000).

The finding of lowered P300 amplitude in sons of alcoholics, a population considered to be at high risk for developing alcoholism, was first reported by Begleiter et al. (1984). The amplitude of P300 is associated more with a family history of alcoholism in alcoholics rather than the amount of alcohol abused (Patterson et al., 1987; Pfefferbaum et al., 1991). Polich et al. (1994), in a meta-analysis of relevant literature, indicated that a paternal history of alcoholism was associated with reduced P300 amplitudes, particularly in male offspring. The results were better defined in studies using tasks in the visual modality. Studies have shown that P300 amplitude is heritable (for a review and meta-analysis, see van Beijsterveldt and van Baal, 2002). Some authors have also shown that smaller P300 amplitudes can predict future substance use and abuse (Berman et al., 1993; Hill et al., 2000; Iacono et al., 2002). The search for endophenotypes for alcoholism using event-related potential (ERP) methodology has uncovered a stable candidate for a trait marker in lowered P300 amplitudes in a visual oddball task (Porjesz et al., 1998; Van der Stelt, 1998, 1999).

The P300 component has multiple distributed generators. On account of varying topographical presentations of P300 for auditory and visual stimuli, it has been suggested that some of the generators may be modality specific, while a few common to both modalities (Ji et al., 1999; Johnson, 1989; Katayama and Polich, 1999). In the investigation of neural generators of P300, significant contributions have come from varying methodologies such as interpretations of brain lesions, source localizations of scalp potentials, intracranial recordings, magnetoencephalography (MEG), functional magnetic resonance imaging (fMRI), and positron emission tomography (PET) (for a review, see Herrmann and Knight, 2001). The literature indicates the involvement of cortical, thalamic, and limbic regions. Of the methodologies listed, fMRI offers a measure of localization of brain activity with good time resolution and hence has contributed extensively to the study of sources of cognitive scalp components such as P300.

Most fMRI studies using the oddball paradigm report consistent activations in bilateral supramarginal gyrus (SMG, BA 40) and anterior cingulate cortex (ACC) irrespective of the task modality (Ardekani et al., 2002; Clark et al., 2000; Kiehl and Liddle, 2001; Linden et al., 1999; McCarthy et al., 1997; Menon et al., 1997; Yoshiura et al., 1999). Studies also report dorsolateral prefrontal cortex (DLPFC) activation quite uniformly but do not concur regarding the laterality of activation (Ardekani et al., 2002; Clark et al., 2000; Kiehl and Liddle, 2001; McCarthy et al., 1997; Yoshiura et al., 1999). Activations in the thalamus and insula are inconsistently reported (Ardekani et al., 2002; Clark et al., 2000; Linden et al., 1999; Menon et al., 1997; Yoshiura et al., 1999). Inferior occipitotemporal cortex activations are also reported (Ardekani et al., 2002; Clark et al., 2000; Yoshiura et al., 1999) and one study reported activation in the cerebellum (Clark et al., 2000).

While electrophysiological paradigms have revealed significant deficits in high-risk offspring of alcoholics, this has not been examined in an analogous event-related brain imaging paradigm.

While existing studies have contributed greatly to our understanding of brain regions underlying the performance of the oddball tasks, there is a paucity of information about the activation profile in an oddball task in subjects at risk for developing alcoholism. In the context of strong evidence for lowered P300 amplitude in high-risk subjects, the present study attempts to explore differences in the structural network for target processing in controls (low risk) and subjects at high risk for developing alcoholism, using functional MRI. The event-related activations are examined using a near full brain coverage and a novel nonparametric randomization-based statistical analysis method (Ardekani et al., 2002).

Materials and methods

Subjects

The subjects in this study consisted of a group of males at high risk for developing alcoholism (HR, $n = 8$) and a low-risk (control) group comprising normal healthy males (LR, $n = 6$) and were in the age range of 21 to 30 years. Except for two LR subjects, all subjects were right handed. LR individuals were recruited either through newspaper ads or via notices posted in the SUNY Health Science Center. The HR subjects had fathers who were undergoing treatment in the Short Term Alcohol Treatment Unit of the Kings County Hospital Center of New York. Initially, each subject filled out a detailed questionnaire concerning the medical and psychiatric histories and alcohol and drug use for both himself and his relatives. Exclusion criteria for this study were (a) personal history of medical or psychiatric problems, (b) maternal alcoholism, and (c) use of psychoactive medication. The low-risk subjects had no first- or second-degree alcoholic relatives. Subject demographic and alcohol use details are summarized in Table 1. Following the selection, subjects underwent neurophysiological assessment in the laboratory. The final selection of the subjects was completed on the basis of the P300 amplitudes obtained from the visual oddball task.

Sixteen male subjects were recruited for this study using a 'psychophysiological high-risk' design (Iacono et al., 2000). The subjects were selected from a large database of control and high-risk individuals based on the following criteria for P300 amplitudes—low risk: subjects with amplitudes higher than the mean amplitude for the entire control group; high risk: subjects having amplitudes lower than the mean amplitude for the entire high-risk population (Table 2 and Fig. 1). The data from two subjects were

Table 1
Summary of demographic and clinical details of low- and high-risk sample

	Low risk (LR)	High risk (HR)
<i>n</i>	6	8
Mean age (in years)	23.3	24.4
Handedness	2—left, 4—right	8—right
Education (average) (number of school years)	14	13
MMSE score (average)	28.5	29
Age at first drink (average)	16	14.5
Max drinks in 24-h period	2.8	3.0
Max drinking days (average) (in the last 6 months)	3	11
Tobacco (smoking)	4—no, 2—yes	2—no, 6—yes
Any other substance use	1—marijuana, 5—none	5—marijuana, 3—none

Table 2
P3 characteristics at the Pz electrode

		Low risk	High risk
Nontarget	<i>n</i>	6	8
	P3 amplitude (μV)	7.64	6.83
Target	P3 amplitude (μV)	20.37	13.08

rejected for reasons to be described in the Target detection rates. Of the 14 remaining subjects, 6 were healthy normal controls (ages 21 to 27; mean age 24.5), the LR group, and 8 were high-risk subjects (ages 21 to 30; mean age 24.75), the HR group. The Institutional Review Board (IRB) of the Nathan Kline Institute and SUNY Health Science Center approved all procedures. Written informed consent was obtained from all participants.

Task

The subjects in this experiment were asked to perform the “classic visual oddball task” during fMRI data collection (Ardekani et al., 2002). In this task, visual stimuli were presented to the subjects at regular interstimulus intervals (ISI). There were two types of stimuli: the standard and the target. The standard visual stimulus occurred more frequently than the target stimulus. The subjects were instructed to silently count the target stimuli and report the total number at the end of the experiment. In the present study, the standard visual stimulus (93.75% of trials) and the target image consisted of a string of white characters on a dark background (Fig. 2). Visual stimuli were delivered to the subject via a liquid crystal display (LCD) mounted on the MRI scanner’s radio frequency (RF) head coil. The LCD display was connected to the video graphics array (VGA) output of a personal computer (PC) outside the scanner room. A total of 1024 images were shown to the subjects (64 targets and 960 standards) in four experimental runs of 256. The interstimulus interval (ISI) was 1648 ms. Stimulus duration was approximately 500 ms. During the remaining time (approximately 1148 ms) the screen was dark. There was a slight delay (less than 10 s) between experimental runs, which was required to reload the MRI scanner pulse sequence. The target events were distributed randomly among the 4 runs and 1024 trials. The temporal structure of the train of stimuli, although randomly selected, was identical across all subjects.

Image acquisition

Images were acquired using a 1.5 T Siemens Vision MRI system (Siemens AG, Erlangen, Germany) located at the Center for

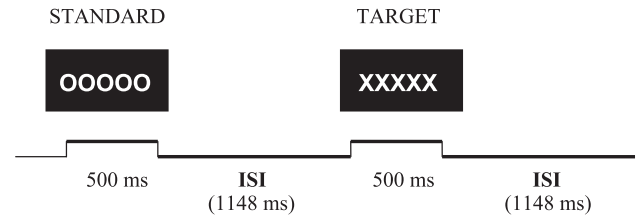


Fig. 2. The two stimuli (standard and target) and task design used in the present fMRI study.

Advanced Brain Imaging of the Nathan Kline Institute. A quadrature head coil was used for RF transmission and reception. The subjects were given earplugs and were positioned supine and comfortably in the magnet. Cushions were placed around the subjects’ head to reduce motion. Scanning began with a number of localizer scans used to orient the functional scans approximately perpendicular to the midsagittal plane and parallel to the line connecting the anterior and posterior commissures (AC–PC line). Blood oxygenation level dependent (BOLD) functional scans were obtained using a T_2^* -weighted gradient echo single-shot echo-planar imaging (EPI) sequence with TR = 1648 ms, TE = 45 ms, flip angle = 90° , and FOV = $250 \times 250 \text{ mm}^2$. A total of 1024 EPI volumes were acquired from each subject. Each volume covered nearly the entire cerebrum and the superior aspect of the cerebellum, consisting of 15 transverse slices of size 64×64 with a pixel size of approximately $3.91 \times 3.91 \text{ mm}^2$ and a slice thickness of 6 mm with no gaps. The acquisition of each EPI volume was synchronized with the onset of a visual stimulus. The synchronization was achieved by triggering the MRI scanner using an external TTL pulse generated by the stimulus presentation PC. In addition to the EPI data, a high-resolution anatomical 3D T_1 -weighted image volume was acquired from each subject using a magnetization-prepared rapid acquisition gradient echo (MP-RAGE) sequence. The scan parameters for this sequence were TR = 11.6 ms, TE = 4.9 ms, flip angle = 8° , FOV = $256 \times 256 \times 190 \text{ mm}^3$, with a matrix size of $256 \times 256 \times 190$ volume elements (voxels), yielding a 1-mm^3 isotropic voxel size.

Two areas of the cerebrum were not covered by the EPI sequence FOV in most subjects: the orbital frontal area and the anterior inferior temporal lobe. The orbital frontal area is generally difficult to image using EPI because of strong susceptibility artifacts. The anterior inferior temporal lobe was not imaged because of the limited number of slices possible to acquire within the TR of the paradigm. Fig. 3 shows the brain areas that were not imaged by the EPI sequence. This image was created by registering the EPI volume to the high-resolution MP-RAGE volume of a typical subject and fusing the registered EPI (color) and MP-RAGE

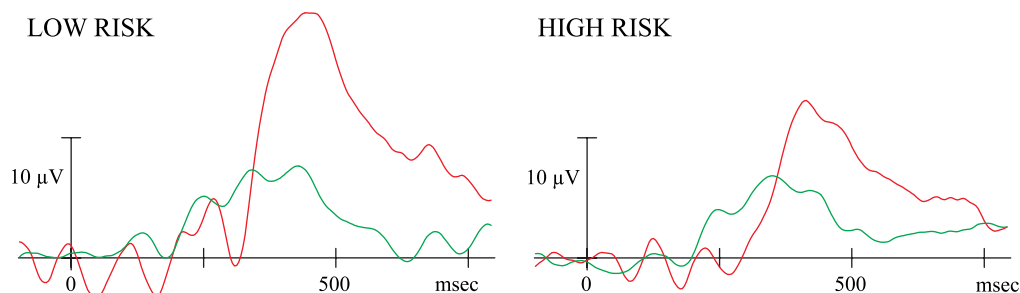


Fig. 1. Visual P300 grandmean waveforms for the two groups. Target waveforms are in red, while the nontarget waveforms are in green.

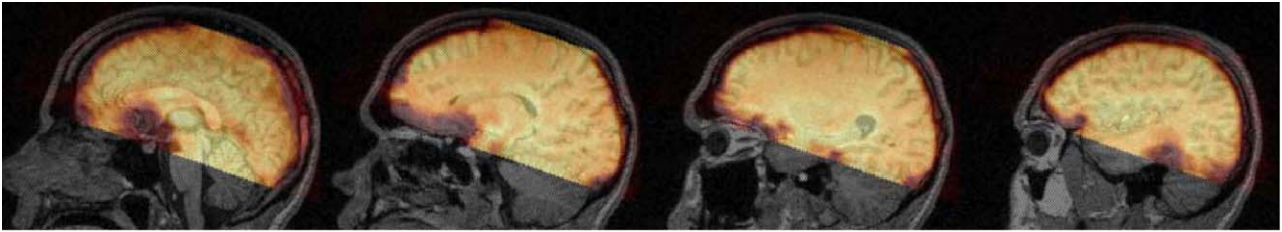


Fig. 3. Fusion of registered EPI (color) and MP-RAGE (gray) images indicating the brain areas that were not imaged by the EPI sequence (cerebellum, inferior temporal lobe) or were affected by signal loss due to susceptibility artifact (orbital frontal area). From left to right, the images correspond to 0, 15, 25, and 40 mm to the left of the midsagittal plane, respectively.

images (gray). From left to right, the slices correspond to 0, 15, 25, and 40 mm to the left of the midsagittal plane, respectively. The areas of the cerebellum and the temporal lobes that were not imaged in the EPI sequence can be seen in this figure. Also, the EPI signal in the orbital frontal area is lost due to the susceptibility artifact as seen on the second image from left.

Image processing

All image processing and analyses were performed on an 800-MHz Dell Precision Workstation 420 computers (Dell Computer Co., Round Rock, TX) running the Red Hat Linux 6.2 operating system (Red Hat Co., Durham, NC). The first four scans from each of the four experimental runs of 256 were discarded to ensure steady state magnetization, leaving a total of 1008 EPI volumes to be analyzed for each subject. Motion detection and correction was performed on the data using the motion correction module of the AFNI software package (Cox, 1996). Accuracy of this motion correction method was validated in a separate study (Ardekani et al., 2001).

After motion correction, the 1008 EPI volumes were averaged and the intracranial region was segmented by thresholding the average image. The threshold was selected automatically by analyzing the image histogram. After thresholding, a connected component analysis was performed that selects the largest four-connected component in the thresholded binary image and removes all other small components. In addition, the largest four-connected component is made simply connected by filling any cavities within it.

Following the definition of the brain mask, the brain voxels' time series were centered to have zero mean. In addition, several "trend" components were regressed out of each time series. The trends were identified by principal component analysis (PCA) of the data from all brain voxels. The number of principal components that were identified and removed from the data sets varied from subject to subject. A heuristic method for identifying the number of components was used, namely, that the component had to explain at least 3% of the total variation in the data and have a cross correlation of less than 0.05 with the reference vector representing the stimulus presentation pattern. This heuristic procedure identified between two and nine components depending on the subject.

Following motion correction and trend removal of the EPI data, the sagittal MP-RAGE images from each subject were spatially registered to the raw axial EPI volumes of the same subject using a six-parameter rigid-body transformation. Since the EPI and MP-RAGE volumes were scanned during the same session, the transformation required for the MP-RAGE to EPI registration was deduced from the header information contained in the Siemens

Vision file format. The resulting axial MP-RAGE images were then transformed into the Talairach stereotactic atlas (Talairach and Tournoux, 1988) using the AFNI software package. The same transformation was then applied to the EPI volumes to transform them into the Talairach coordinates. The transformed EPI volumes were resampled to a voxel size of $3 \times 3 \times 3 \text{ mm}^3$ and a matrix size of $54 \times 64 \times 50$. We then computed two medians, one for the six data sets corresponding to the LR group and the other for the eight data sets belonging to the HR group. The median is immune to outliers and avoids the situation where a strong region of activation in a single subject may be incorrectly attributed to the entire group. We then analyzed each of the two median data sets separately to obtain activation maps for the two groups of subjects. We also determined statistically significant differences between the two activation maps.

Statistical analysis of within-group median data sets

Nonparametric randomization-based statistical methods were employed for detecting the activated brain regions within each group. In this method, the data are essentially analyzed N times (for the present paper, $N = 1000$). The following steps are performed in each of the N analyses:

- (1) Let K represent the total number scans or trials. In this paper, $K = 1008$. By random sampling without replacement, select T of the K trials, where T is the number of target events (in this case 64). Thus, from the set of integers $\{1, 2, \dots, K\}$, a random subset of size T is selected at this step of the analysis. The random selection routine used in this step is the same method used for setting the actual temporal structure of time points where the target stimuli were shown to the subjects in the fMRI experiments.
- (2) Let the times (in seconds) corresponding to the T randomly selected trials in Step 1 be denoted by $\{t_1, t_2, \dots, t_T\}$. Compute the expected BOLD response function as follows:

$$r(t) = \sum_{i=1}^T h(t - t_i) \quad (1)$$

where $h(t)$ is a model for the hemodynamic impulse response function given by:

$$h(t) = \begin{cases} e^{-t/\sqrt{\delta\tau}} \left(\frac{e t}{\tau}\right) \sqrt{\tau/\delta} & t > 0 \\ 0 & t < 0 \end{cases} \quad (2)$$

The parameter $\tau = 4.7 \text{ s}$ marks the peak of the impulse response function, and $\delta = 0.06$ is a dimensionless parameter

that controls its shape. Sample $r(t)$ at a K regular time points $t_n = n \times TR$ to form the reference vector:

$$\mathbf{r} = [r(0) \ r(TR) \ \dots \ r((K-1)TR)]^T$$

and finally normalize the reference vector \mathbf{r} to obtain $\hat{\mathbf{r}}$.

- (3) Let \mathbf{x}_n represent the time series of length K at voxel n in the median data set. For each voxel, compute the statistic:

$$s_n = \frac{\mathbf{x}_n \cdot \hat{\mathbf{r}}}{\sqrt{\mathbf{x}_n \cdot \mathbf{x}_n - (\mathbf{x}_n \cdot \hat{\mathbf{r}})^2}} \quad (3)$$

This statistic is the cotangent of the angle between the fMRI time series vector \mathbf{x}_n and the zero-mean normalized reference vector $\hat{\mathbf{r}}$. The reference vector models the changes in image intensity that we expect to observe based on the assumed experimental stimulation paradigm.

- (4) Find the maximum value of s_n across the image: $s_{\max} = \max(s_n)$.
- (5) Repeat Steps 1 to 4 N times to obtain an empirical distribution for the maximal statistic s_{\max} .
- (6) Finally, analyze the data using Steps 1 to 3 one last time with the actual stimulus pattern used in the experiment. In this case, the times $\{t_1, t_2, \dots, t_T\}$ are not select randomly. They are the actual times when the target events were presented to the subjects. Thus, we obtain a statistical map with a value of s_n at each voxel. In this map, all voxels for which the test statistic s_n falls within the top α percentile of the empirically determined probability distribution function of the maximal test statistic s_{\max} obtained in Step 5 are declared activated.

It can be shown that the test described above controls for multiple comparisons. That is, if in reality no voxel is activated anywhere in the brain, the probability that at least one voxel somewhere in the brain is (falsely) declared activated by the activation detection test is at most equal to α .

Note that in randomization procedure outlined above, the order of the scans in time is not altered, and therefore any existing temporal correlation in the data remains intact. Randomization is only performed on times of occurrences of the target events.

Statistical analysis of group differences

The procedure for determining the statistically significant differences between the activation patterns of the two groups of subjects is exactly as described above, except that a different test statistic, d_n , is used, which is defined as follows:

$$d_n = \begin{cases} s_{1n} & \text{if } s_{2n} < 0 \\ s_{1n} - s_{2n} & \text{otherwise} \end{cases} \quad (4)$$

where s_{1n} and s_{2n} are the test statistics computed from Eq. (3) for median data sets corresponding to Groups 1 and 2, respectively. This statistic indicates voxels that are significantly more activated in Group 1 relative to Group 2. In the absence of the “if” condition in Eq. (4), it is conceivable that a voxel with a small positive or even a negative s_{1n} value and a negative s_{2n} value with a large magnitude would be classified as being significantly more “activated” in Group 1 as compared to Group 2; whereas in fact, the voxel cannot be called active in Group 1. An advantage of

permutation-based analysis methods is that this type of nonlinearity can be readily incorporated into the definition of the test statistic.

Results

Target detection rates

The average error magnitude was 2.833 for the low-risk group and 2.875 for the high-risk group. One LR subject detected 235 targets and one HR subject detected 98 targets. Given that there were only 64 true targets in the oddball paradigm, the excessive number of false alarms by these subjects was an indication that they had not followed the instructions given to them prior to the experiment. Consequently, these subjects were excluded from further analysis. The remaining six LR and eight HR subjects were analyzed for presence of brain activation, the results of which are presented below.

Within-group activations

The resulting patterns of activations ($P < 0.05$; corrected for multiple comparisons) for the low- and high-risk groups were remarkably similar (Figs. 4–6). There were three common regions activated in the two groups: (1) the anterior cingulate gyrus (BA 32) (Fig. 4); (2) the bilateral inferior parietal lobule (BA 40; (Fig. 5); and (3) the bilateral anterior insula (Fig. 6). The low-risk group additionally activated the posterior cingulate (BA 23) and the bilateral inferior frontal gyrus (BA 44) (Fig. 7). Lowering the threshold of the activation map in the high-risk group did show activity in the posterior cingulate. However, this activation was not statistically significant.

Between-group activations

Two areas showed significantly lower activation in the HR group as compared to the LR group ($P < 0.05$; corrected for multiple comparisons): the bilateral inferior parietal lobule (BA 40) (Fig. 8a), and the bilateral inferior frontal gyrus (BA 44) (Fig. 8b). A significant difference between the activation in the two groups could arise in two different ways. First, an area may be activated in both groups, but the activation may be significantly lower in one group as compared to the other. This is the case for the activation of the angular gyrus of the inferior parietal lobule (Fig. 4). Parietal lobe activation is present in both LR and HR groups. However, activation in the HR group is significantly lower than that of the LR group. On the other hand, significant differences between group activations may arise because an area was activated in one group but not in the other group. This was the case with the inferior frontal gyrus activation, which was activated only in the LR group but not in the HR group (Fig. 7).

Discussion

The results reveal that detection of the infrequent target stimuli produced similar patterns of activations in HR and LR (control) subjects. The LR subjects activated the anterior cingulate gyrus (ACC); inferior parietal lobule, bilaterally (BA 40); anterior insula, bilaterally; posterior cingulate (PCC); and bilateral inferior frontal gyrus (BA 44). The pattern of activation was similar for the HR

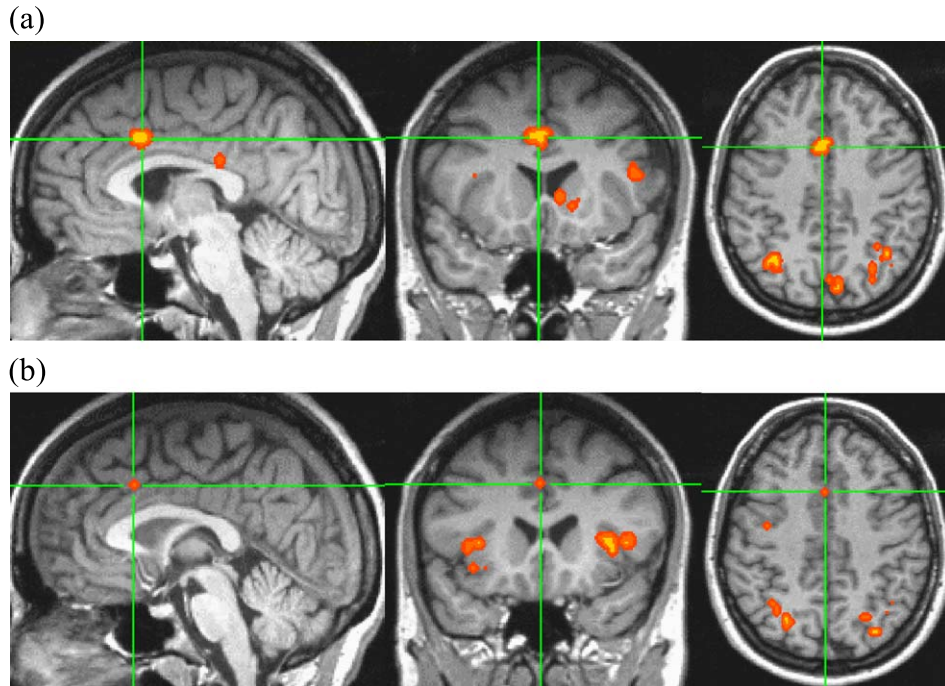


Fig. 4. Anterior cingulate gyrus activation in (a) the low-risk group and (b) the high-risk group ($P < 0.05$; corrected for multiple comparisons).

subjects with two notable differences. The HR group showed no activation in the inferior frontal gyrus bilaterally, and the activation of inferior parietal lobule (BA 40) was significantly lower in HR subjects when compared to LR subjects. Although visual inspection of the images showed lower activation in ACC for the HR subjects, the observation did not reach statistical significance (Fig. 4). Also,

activation in the PCC in HR subjects was observed only when the threshold of activation map was lowered.

The present study reveals activation patterns in LR subjects similar to other fMRI studies on visual target detection tasks (Ardekani et al., 2002; Clark et al., 2000; Yoshiura et al., 1999). However, the results highlight two issues: (a) all differences

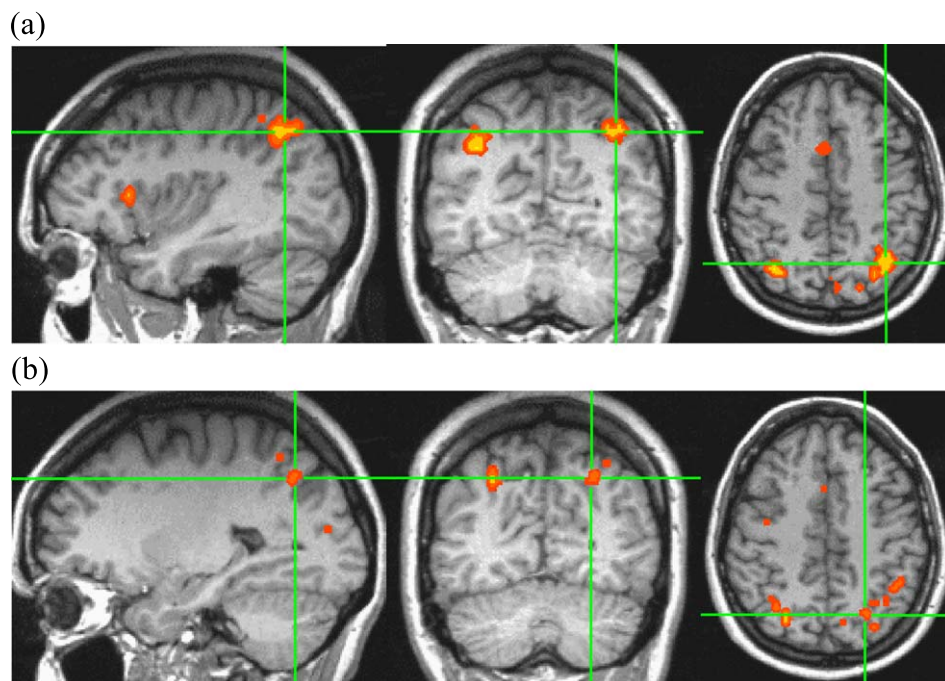


Fig. 5. Activation of the bilateral inferior parietal lobule in (a) the low-risk group and (b) the high-risk group ($P < 0.05$; corrected for multiple comparisons).

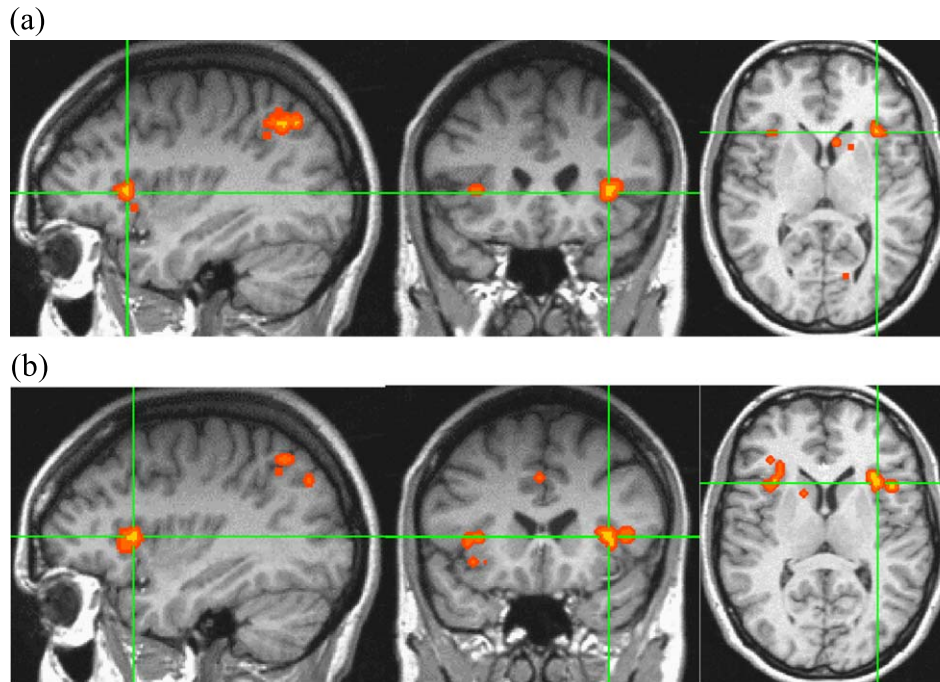


Fig. 6. Bilateral activation of the anterior insula in (a) the low-risk group and (b) the high-risk group ($P < 0.05$; corrected for multiple comparisons).

observed between HR and LR subjects were bilateral; and (b) subtle differences from other localization studies of visual P300. The attentional and memory updating functions ascribed to the P300 components of the visual discrimination task engage both hemispheres. This view is supported by an absence of lateralized P300

responses to unilateral field stimulation (Clarke et al., 1999) and unilateral lesions studies (Knight et al., 1989). The results of the present study appear to follow this trend.

Halgren et al. (1995) have suggested that in the commonly employed cognitive tasks using the subtraction technique, areas

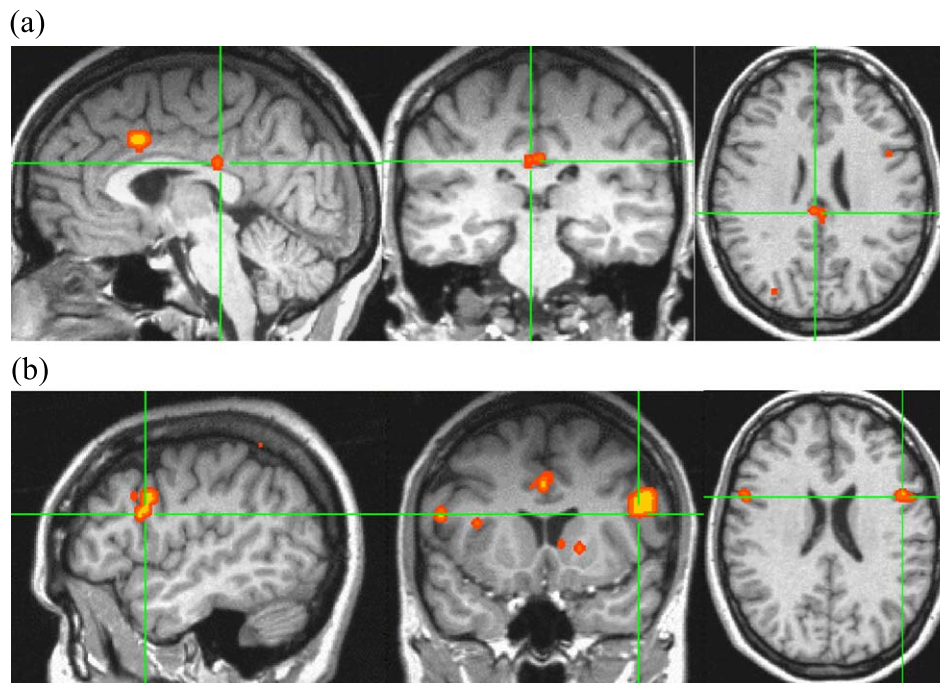


Fig. 7. Posterior cingulate activation (a) and bilateral inferior frontal gyrus activation (b) were detected in the low-risk group but not the high-risk group ($P < 0.05$; corrected for multiple comparisons). Lowering the threshold of the activation map in the risk group did show activity in the posterior cingulate. This activation was not statistically significant.

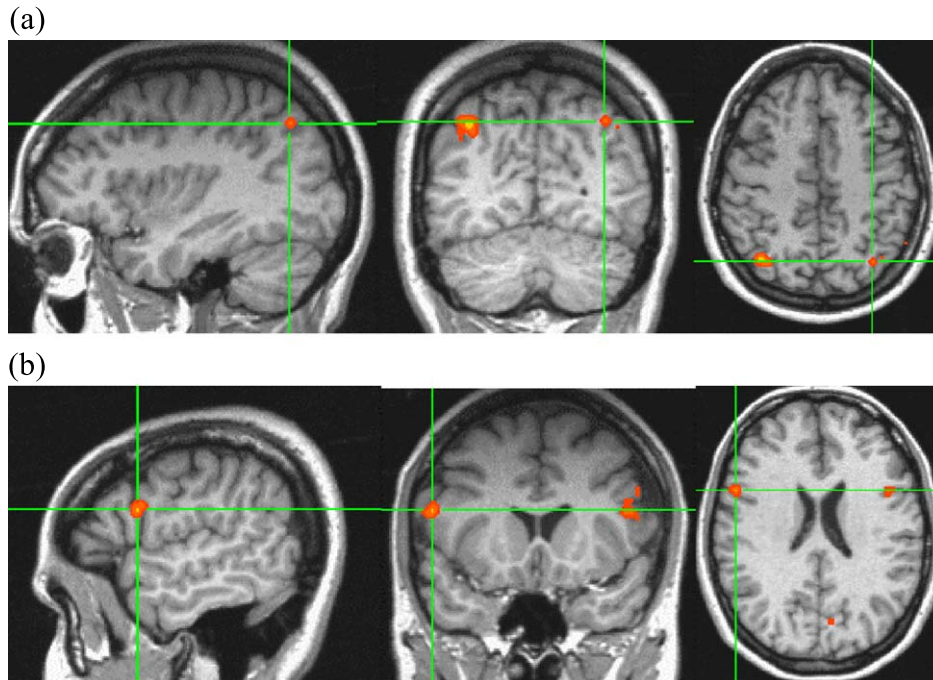


Fig. 8. Two areas showed significantly greater activation in the low-risk group as compared to the high-risk group: (a) the bilateral angular gyrus of the inferior parietal lobule, and (b) the bilateral inferior frontal gyrus ($P < 0.05$; corrected for multiple comparisons).

essential in the ‘active’ task may be engaged even during the ‘baseline’ task. In which case, the active areas would be subtracted out even when they may be required for the ‘active’ task. This could be an important issue that concerns the variability in activated regions reported in the various studies on visual P300 processing. The variations in regional activations reported in fMRI studies on P300 can also be the result of differences in (a) stimulation paradigm (type of sensory stimulus, frequency of rare events, and number of trials), (b) scanning parameters (slice thickness, repetition time, and brain coverage), and (c) statistical analysis method employed. These issues have been discussed in detail, in the context of the methodology used in the present study, elsewhere (Ardekani et al., 2002).

In the context of the scalp recorded P300 deficit that has been widely reported in the HR subjects, the results of the present study provide an anatomical and conceptual basis of the phenomenon. The inclusion of HR subjects in the study was based on their low P300 values that were obtained during electrophysiological testing prior to the fMRI (Table 2). It is likely that the P300 amplitude deficit observed in the scalp recording of these HR subjects may be a function of reduced activations of the supramarginal gyrus (SMG; BA 40) and inferior frontal gyrus (BA 44).

Inferior frontal gyrus (BA 44/6) activation has been reported in studies on verbal working memory and in particular for phonological processing (Awh et al., 1996; Jonides et al., 1998; McDermott et al., 2003; Paulesu et al., 1993). The studies indicate this region to be an important relay in the rehearsal system of working memory. Contributions of the activity in the inferior frontal gyrus to the scalp recorded P300 can be speculated. In visual tasks employing three or more types of stimuli, the P300 component can be separated into a more frontal and early P300a and a temporoparietal P300b. One study reported large intracerebral P300 as that were recorded laterally, especially near the inferior frontal sulcus, and clear

inversions of the P300a were also noted in the orbitofrontal and the anterior cingulate cortices (Baudena et al., 1995). Intracranial recordings in prefrontal cortical areas (including dorsal superior, middle, and/or inferior frontal gyri) revealed the presence of both early and late P300-like components around 350 and 550 ms, respectively (Clarke et al., 1999).

The lowered activation in ACC and no activation in the inferior frontal gyrus for the HR subjects are possibly related. The inferior frontal gyrus (BA 44) has extensive reciprocal connections with ACC (Joseph, 1990). It is possible that activation in the ACC is influenced by the nonengagement of the inferior frontal gyrus in this task-related circuitry.

Convergent findings from intracerebral recordings of P300 and fMRI studies provide significant evidence for the activation of SMG during target detection (Ardekani et al., 2002; Clark et al., 2000; Linden et al., 1999; McCarthy et al., 1997; Menon et al., 1997). Unilateral lesions to the temporoparietal cortex have been shown to abolish scalp P300b (Knight et al., 1989). Menon et al. (1997) speculated that the dominant contribution to the scalp P300b arises from bilateral activation of superficial sources in the supramarginal gyrus, roughly in the interval of 285 to 610 ms following the target stimulus onset.

Greicius et al. (2003) suggest that task-related activation in PCC can be detected only when the experimental condition is contrasted with an equally complex baseline condition since the PCC functions as an important node in the default mode network. A default mode network consists of networks that are more active in the resting or control state than the experimental state; hence, some regions show deactivations in standard fMRI protocols. PCC is one such region and some studies have observed deactivation in PCC during cognitive tasks (Mazoyer et al., 2001; Raichle et al., 2001). More supporting evidence comes from a study showing activation of PCC in episodic memory retrieval when contrasted with a complex

baseline, as opposed to mere visual fixation baseline (Cabeza et al., 2002). Two studies report PCC activation in visual oddball task (Ardekani et al., 2002; McCarthy et al., 1997) where the experimental condition (infrequent visual stimulus) was contrasted with a complex baseline (frequent visual stimulus). In the present study, PCC activation is seen in LR, but in HR it appears only when the threshold of activation map is lowered. This suggests that the default mode in HR individuals may be comparable to the LR subjects, but the task-related recruitment of PCC is not adequate, or more likely the HR subjects use default mode circuits in both conditions. This is consistent with electrophysiological evidences of undifferentiated mode of functioning that has been well documented in alcoholics and individuals at risk (Porjesz and Begleiter, 1995, 1996, 1997).

Neuroanatomical substrates of P300 and working memory

McCarthy et al. (1997) provide strong evidence, which suggests that components of the neural system mediating working memory, identified in previous neuroimaging studies in humans and in single-unit recordings in monkeys, may be activated by the same events that evoke P300 (Cohen et al., 1994; McCarthy et al., 1994, 1996; Smith et al., 1995). Key areas of activation include middle frontal gyri and inferior parietal lobe, both bilaterally and posterior cingulate gyrus.

Working memory allows one to maintain a limited amount of information in an active store for a short time and manipulate it (Baddeley, 1992). In a model of human working memory, separate systems handling verbal and spatial information have been conceptualized, supported by neuroimaging evidences (Smith and Jonides, 1998). Both systems have been proposed to comprise three functional components: (1) a pure storage component, (2) a rehearsal component, and (3) an executive component. According to the model of verbal working memory segment after visual encoding, the targets are translated into phonological representations in inferior frontal, superior temporal, and posterior parietal areas. These phonological representations are kept in active storage in the posterior parietal region, and the storage is maintained by constant rehearsal that involves the Broca's area (frontal speech area, BA 44). In a recent study, activations were noted in Broca's area and left angular gyrus when nonmanipulable objects were held in working memory (Mecklinger et al., 2002). The spatial system is mediated by a similar network, predominantly in the right hemisphere, and includes areas in the posterior parietal, occipital, and frontal cortex. Suggestive evidence for right posterior parietal (BA 40) and right premotor areas serving as storage and rehearsal regions for spatial working memory comes from neurological and fMRI evidence from item recognition tasks (Jonides et al., 1993; Smith and Jonides, 1998).

The task used in the present study comprised visual stimuli that could easily be verbalized. In addition, the subjects were instructed to keep a mental count of the number of targets events. This task involved more of information maintenance rather than information manipulation. All subjects included in the study complied with the task demand as indicated by the target event counts. The results of the present study show no activation in the inferior frontal gyrus in HR subjects, an area involved in the rehearsal system of working memory. This indicates an ineffective activation of the rehearsal system of the working memory in HR subjects. Any deficiency in the updating function is likely to weaken the activation in the

storage region. SMG (BA 40) is the locus of the phonological store that is constantly updated by the rehearsal system (Vallar et al., 1997). Hence, the reduced activation of SMG or inferior parietal when compared to LR subjects can also be linked to the ineffective functioning of rehearsal system.

Conclusion

The present study demonstrates that LR subjects employ distributed networks to accomplish the task, while the HR subjects appear to utilize minimal neural substrates. It is possible that the HR subjects have adopted a less optimal or a different strategy to perform the task and the frontoparietal circuits are not utilized optimally. HR subjects and alcoholics have been reported to manifest undifferentiated responses to targets and nontargets (Porjesz and Begleiter, 1995, 1996, 1997). This study suggests that HR subjects possibly employ fewer distributed networks when compared to LR subjects to accomplish the same task. The reduced P300 observed in HR subjects could be a result of a less than optimal functioning of the frontoparietal circuits, which contributes to a lowered efficiency of neural processing. The cognitive correlate of these indicates deficient rehearsal in the working memory functions involved in this task. Although, we must exercise a certain amount of caution in interpreting these results, especially in view of the sample size, the psychophysiological high-risk design used in the present study aids in sharpening group differences. Future studies are needed to demonstrate and examine structural and functional (excitatory and inhibitory transmitters; receptors) contributors of the lack of coupling of associated networks utilized in this task in HR subjects.

Acknowledgments

The authors thank Arthur T. Stimus for valuable technical support. This research was supported by the grant number NIAAA12560 from the National Institute on Alcohol Abuse and Alcoholism.

References

- Ardekani, B.A., Bachman, A.H., Helpem, J.A., 2001. A quantitative comparison of motion detection algorithms in fMRI. *Magn. Reson. Imaging* 19, 959–963.
- Ardekani, B.A., Choi, S.J., Hossein-Zadeh, G.A., Porjesz, B., Tanabe, J.L., Lim, K.O., Bilder, R., Helpem, J.A., Begleiter, H., 2002. Functional magnetic resonance imaging of the brain activity in the visual oddball task. *Brain Res. Cogn. Brain Res.* 14 (3), 347–356.
- Awh, E., Jonides, J., Smith, E.E., Schumacher, E.H., Koeppel, R.A., Katz, S., 1996. Dissociation of storage and rehearsal in verbal working memory. *Psychol. Sci.* 7 (1), 25–31.
- Baddeley, A., 1992. Working memory. *Science* 255 (5044), 556–559.
- Baudena, P., Halgren, E., Heit, G., Clarke, J.M., 1995. Intracerebral potentials to rare target and distractor auditory and visual stimuli: III. Frontal cortex. *Electroencephalogr. Clin. Neurophysiol.* 94 (4), 251–264.
- Begleiter, H., Porjesz, B., Bihari, B., Kissing, B., 1984. Event-related potentials in boys at risk for alcoholism. *Science* 225, 1493–1496.
- Berman, S.M., Whipple, S.C., Fitch, R.J., Noble, E.P., 1993. P3 in young boys as a predictor of adolescent substance use. *Alcohol* 10 (1), 69–76.

- Cabeza, R., Dolcos, F., Graham, R., Nyberg, L., 2002. Similarities and differences in the neural correlates of episodic memory retrieval and working memory. *Neuroimage* 16 (2), 317–330.
- Clark, V.P., Fannon, S., Lai, S., Benson, R., Bauer, L., 2000. Responses to rare visual target and distractor stimuli using event-related fMRI. *J. Neurophysiol.* 83, 3133–3139.
- Clarke, J.M., Halgren, E., Chauvel, P., 1999. Intracranial ERPs in humans during a lateralized visual oddball task: II. Temporal, parietal, and frontal recording. *Clin. Neurophysiol.* 110 (7), 1226–1244.
- Cohen, J.D., Forman, S.D., Braver, T.S., Casey, B.J., Servan-Schreiber, D., Noll, D.C., 1994. Activation of prefrontal cortex in a non-spatial working memory task with functional MRI. *Hum. Brain Mapp.* 1, 293–304.
- Cox, R.W., 1996. AFNI: software for analysis and visualization of functional magnetic resonance neuroimages. *Comput. Biomed. Res.* 29, 162–173.
- Donchin, E., Coles, M.G.H., 1988. Is the P300 component a manifestation of context updating? *Behav. Brain Sci.* 11, 357–374.
- Duncan-Johnson, C.C., Donchin, E., 1977. On quantifying surprise: the variation of event-related potentials with subjective probability. *Psychophysiology* 14 (5), 456–467.
- Greicius, M.D., Krasnow, B., Reiss, A.L., Menon, V., 2003. Functional connectivity in the resting brain: a network analysis of the default mode hypothesis. *Proc. Natl. Acad. Sci. U. S. A.* 100 (1), 253–258.
- Halgren, E., Baudena, P., Clarke, J.M., Heit, G., Marinkovic, K., Devaux, B., Vignal, J.P., Biraben, A., 1995. Intracerebral potentials to rare target and distractor auditory and visual stimuli: II. Medial, lateral and posterior temporal lobe. *Electroencephalogr. Clin. Neurophysiol.* 94 (4), 229–250.
- Herrmann, C.S., Knight, R.T., 2001. Mechanisms of human attention: event-related potentials and oscillations. *Neurosci. Biobehav. Rev.* 25 (6), 465–476.
- Hill, S.Y., De Bellis, M.D., Keshavan, M.S., Lowers, L., Shen, S., Hall, J., Pitts, T., 2001. Right amygdala volume in adolescent and young adult offspring from families at high risk for developing alcoholism. *Biol. Psychiatry* 49 (11), 894–905.
- Hill, S.Y., Shen, S., Lowers, L., Locke, J., 2000. Factors predicting the onset of adolescent drinking in families at high risk for developing alcoholism. *Biol. Psychiatry* 48 (4), 265–275.
- Iacono, W.G., Carlson, S.R., Malone, S.M., 2000. Identifying a multivariate endophenotype for substance use disorders using psychophysiological measures. *Int. J. Psychophysiol.* 38 (1), 81–96.
- Iacono, W.G., Carlson, S.R., Malone, S.M., McGue, M., 2002. P3 event-related potential amplitude and the risk for disinhibitory disorders in adolescent boys. *Arch. Gen. Psychiatry* 59 (8), 750–757.
- Ji, J., Porjesz, B., Begleiter, H., Chorlian, D., 1999. P300: the similarities and differences in the scalp distribution of visual and auditory modality. *Brain Topogr.* 11 (4), 315–327.
- Johnson Jr., R., 1989. Developmental evidence for modality-dependent P300 generators: a normative study. *Psychophysiology* 26 (6), 651–667.
- Jonides, J., Smith, E.E., Koeppe, R.A., Awh, E., Minoshima, S., Mintun, M.A., 1993. Spatial working memory in humans as revealed by PET. *Nature* 363 (6430), 623–625.
- Jonides, J., Schumacher, E.H., Smith, E.E., Koeppe, R.A., Awh, E., Reuter-Lorenz, P.A., Marshuetz, C., Willis, C.R., 1998. The role of parietal cortex in verbal working memory. *J. Neurosci.* 18 (13), 5026–5034.
- Joseph, R., 1990. *Neuropsychology, Neuropsychiatry, Behavioral Neurology*. Plenum, New York.
- Katayama, J., Polich, J., 1999. Auditory and visual P300 topography from a 3 stimulus paradigm. *Clin. Neurophysiol.* 110 (3), 463–468.
- Kiehl, K.A., Liddle, P.F., 2001. An event-related functional magnetic resonance imaging study of an auditory oddball task in schizophrenia. *Schizophr. Res.* 48, 159–171.
- Knight, R.T., Scabini, D., Woods, D.L., Clayworth, C.C., 1989. Contributions of temporal-parietal junction to the human auditory P3. *Brain Res.* 502 (1), 109–116.
- Linden, D.E.J., Prvulovic, D., Formisano, E., Völlinger, M., Zanella, F.E., Goebel, R., Dierks, T., 1999. The functional neuroanatomy of target detection: an fMRI study of visual and auditory oddball tasks. *Cereb. Cortex* 9, 815–823.
- Mazoyer, B., Zago, L., Mellet, E., Bricogne, S., Etard, O., Houde, O., Crivello, F., Joliot, M., Petit, L., Tzourio-Mazoyer, N., 2001. Cortical networks for working memory and executive functions sustain the conscious resting state in man. *Brain Res. Bull.* 54 (3), 287–298.
- McCarthy, G., Blamire, A.M., Puce, A., Nobre, A.C., Bloch, G., Hyder, F., Goldman-Rakic, P., Shulman, R.G., 1994. Functional magnetic resonance imaging of human prefrontal cortex activation during a spatial working memory task. *Proc. Natl. Acad. Sci. U. S. A.* 91 (18), 8690–8694.
- McCarthy, G., Puce, A., Constable, R.T., Krystal, J.H., Gore, J.C., Goldman-Rakic, P., 1996. Activation of human prefrontal cortex during spatial and nonspatial working memory tasks measured by functional MRI. *Cereb. Cortex* 6 (4), 600–611.
- McCarthy, G., Luby, M., Gore, J., Goldman-Rakic, P., 1997. Infrequent events transiently activate human prefrontal and parietal cortex as measured by functional MRI. *J. Neurophysiol.* 77 (3), 1630–1634.
- McDermott, K.B., Petersen, S.E., Watson, J.M., Ojemann, J.G., 2003. A procedure for identifying regions preferentially activated by attention to semantic and phonological relations using functional magnetic resonance imaging. *Neuropsychologia* 41 (3), 293–303.
- Mecklinger, A., Ullsperger, P., 1993. P3 varies with stimulus categorization rather than probability. *Electroencephalogr. Clin. Neurophysiol.* 86 (6), 395–407.
- Mecklinger, A., Gruenewald, C., Besson, M., Magnie, M.N., Von Cramon, D.Y., 2002. Separable neuronal circuitries for manipulable and non-manipulable objects in working memory. *Cereb. Cortex* 12 (11), 1115–1123.
- Menon, V., Ford, J.M., Lim, K.O., Glover, G.H., Pfefferbaum, A., 1997. Combined event-related fMRI and EEG evidence for temporal-parietal cortex activation during target detection. *NeuroReport* 8, 3029–3037.
- Nasman, V.T., Rosenfeld, J.P., 1990. Parietal P3 response as an indicator of stimulus categorization: increased P3 amplitude to categorically deviant target and nontarget stimuli. *Psychophysiology* 27 (3), 338–350.
- Nixon, S.J., Tivis, L.J., 1997. Neuropsychological responses in COA's. *Alcohol Health Res. World* 21 (3), 232–236.
- Nixon, S.J., Tivis, R., Parsons, O.A., 1995. Behavioral dysfunction and cognitive efficiency in male and female alcoholics. *Alcohol Clin. Exp. Res.* 19 (3), 577–581.
- Oscar-Berman, M., Hutner, N., 1993. Frontal lobe changes after chronic alcohol ingestion. In: Hunt, W.A., Nixon, S.J. (Eds.), *Alcohol-Induced Brain Damage*. NIAAA Research Monographs, vol. 22. National Institutes of Health, Rockville, MD, pp. 121–156.
- Patterson, B.W., Williams, H.L., McLean, G.A., Smith, L.T., Schaeffer, K.W., 1987. Alcoholism and family history of alcoholism: effects on visual and auditory event-related potentials. *Alcohol* 4, 265–274.
- Paulesu, E., Frith, C.D., Frackowiak, R.S., 1993. The neural correlates of the verbal component of working memory. *Nature* 362 (6418), 342–345.
- Pfefferbaum, A., Ford, J.M., White, P.M., Mathalon, D., 1991. Event-related potentials in alcoholic men: P3 amplitude reflects family history but not alcohol consumption. *Alcohol Clin. Exp. Res.* 15, 839–850.
- Pfefferbaum, A., Desmond, J.E., Galloway, C., Menon, V., Glover, G.H., Sullivan, E.V., 2001. Reorganization of frontal systems used by alcoholics for spatial working memory: an fMRI study. *Neuroimage* 14 (1 Pt 1), 7–20.
- Polich, J., Bondurant, T., 1997. P300 sequence effects, probability and interstimulus interval. *Physiol. Behav.* 61 (6), 843–849.
- Polich, J., Herbst, K.L., 2000. P300 as a clinical assay: rationale, evaluation, and findings. *Int. J. Psychophysiol.* 38 (1), 3–19.
- Polich, J., Pollock, V.E., Bloom, F.E., 1994. Meta-analysis of P300 amplitude from males at risk for alcoholism. *Psychol. Bull.* 115 (1), 55–73.
- Porjesz, B., Begleiter, H., 1995. Event related potentials and cognitive function in alcoholism. *Alcohol Health Res. World* 19, 108–112.
- Porjesz, B., Begleiter, H., 1996. Effects of alcohol on electrophysiological activity of the brain. In: Begleiter, H., Kissin, B. (Eds.), *Alcohol and Alcoholism*. The Pharmacology of Alcohol and Alcohol Dependence, vol. 2. Oxford Univ. Press, New York, pp. 207–247.

- Porjesz, B., Begleiter, H., 1997. Event related potentials in COA'S. *Alcohol Health Res. World* 21, 236–240.
- Porjesz, B., Begleiter, H., Reich, T., Van Eerdewegh, P., Edenberg, H.J., Foroud, T., Goate, A., Litke, A., Chorlian, D.B., Stimus, A., Rice, J., Blangero, J., Almas, L., Sorbell, J., Bauer, L.O., Kuperman, S., O'Connor, S.J., Rohrbaugh, J., 1998. Amplitude of visual P3 event-related potential as a phenotypic marker for a predisposition to alcoholism: preliminary results from the COGA project. *Alcohol Clin. Exp. Res.* 22, 1317–1323.
- Raichle, M.E., MacLeod, A.M., Snyder, A.Z., Powers, W.J., Gusnard, D.A., Shulman, G.L., 2001. A default mode of brain function. *Proc. Natl. Acad. Sci. U. S. A.* 98 (2), 676–682.
- Smith, E.E., Jonides, J., 1998. Neuroimaging analyses of human working memory. *Proc. Natl. Acad. Sci. U. S. A.* 95 (20), 12061–12068.
- Smith, E.E., Jonides, J.M., Koeppe, R.A., Awh, E., Schumacher, E.H., Minoshima, S., 1995. Spatial versus object working memory: PET investigations. *J. Cogn. Neurosci.* 7 (3), 337–356.
- Sullivan, E.V., Mathalon, D.H., Zipursky, R.B., Kerstein-Tucker, Z., Knight, R.T., Pfefferbaum, A., 1993. Factors of the Wisconsin Card Sorting Test as measures of frontal-lobe function in schizophrenia and in chronic alcoholism. *Psychiatry Res.* 46 (2), 175–199.
- Sutton, S., Braren, M., Zubin, J., John, E.R., 1965. Evoked potentials correlates of stimulus uncertainty. *Science* 150, 1187–1188.
- Talairach, J., Tournoux, P., 1988. *Co-Planar Stereotaxic Atlas of the Human Brain*. Georg Thieme Verlag, New York.
- Vallar, G., Di Betta, A.M., Silveri, M.C., 1997. The phonological short-term store-rehearsal system: patterns of impairment and neural correlates. *Neuropsychologia* 35 (6), 795–812.
- van Beijsterveldt, C.E., van Baal, G.C., 2002. Twin and family studies of the human electroencephalogram: a review and a meta-analysis. *Biol. Psychol.* 61 (1–2), 111–138.
- Van der Stelt, O., 1998. The P3 component of the human event-related potential as a vulnerability marker of alcoholism. *Alcohol Res.* 3, 6–9.
- Van der Stelt, O., 1999. Visual P3 as a potential vulnerability marker of alcoholism: evidence from the Amsterdam study of children of alcoholics. *Alcohol* 34, 267–282.
- Verleger, R., 1988. Event-related potentials and cognition: a critique of the context updating hypothesis and an alternative interpretation of P3. *Behav. Brain Sci.* 11, 343–356.
- Volkow, N.D., Wang, G.J., Begleiter, H., Hitzemann, R., Pappas, N., Burr, G., Pascani, K., Wong, C., Fowler, J.S., Wolf, A.P., 1995. Regional brain metabolic response to lorazepam in subjects at risk for alcoholism. *Alcohol Clin. Exp. Res.* 19 (2), 510–516.
- Yoshiura, T., Zhong, J., Shibata, D.K., Kwok, W.E., Shrier, D.A., Numaguchi, Y., 1999. Functional MRI study of auditory and visual oddball tasks. *NeuroReport* 10, 1683–1688.